Plasmon-Enhanced Electron Acceleration in Intense Laser Metal-Cluster Interactions

Th. Fennel,* T. Döppner, J. Passig, Ch. Schaal, J. Tiggesbäumker, and K.-H. Meiwes-Broer

Institut für Physik, Universität Rostock, 18051 Rostock, Germany

(Received 25 September 2006; published 4 April 2007)

We have measured the energy and angular-resolved electron emission from medium-sized silver clusters ($N \simeq 500$–2000) exposed to dual laser pulses of moderate intensity ($I \sim 10^{13-14}$ W/cm^2). When the second pulse excites the plasmon resonantly, we observe enhanced emission along the laser polarization axis. The asymmetry of the electron spectrum is strongly increasing with electron energy. Semiclassical simulations reveal the following mechanism: Electrons bound in highly excited states can leave, return to, and traverse the cluster. Those electrons that return at zero plasmon deflection and traverse the cluster during a favorable plasmon half-cycle can experience maximum acceleration by the evolving polarization field. As a result of these constraints energetic electrons are emitted in direction of the laser polarization axis in subcycle bursts.

DOI: 10.1103/PhysRevLett.98.143401 PACS numbers: 36.40.Gk, 31.15.Gy, 52.50.Jm, 52.65.Rr

Gas-phase clusters are fascinating objects to explore strong-field light-matter interactions in the transition region between the molecular and the solid phase [1]. They absorb intense laser radiation with huge cross sections [2] and emit fast electrons [3,4], energetic photons [5], charged ions [6] with MeV kinetic energy [7–9], and even neutrons [10]. Besides fundamental relevance, also potential applications, e.g., extreme ultraviolet light sources, compact particle accelerators, or pulsed neutron sources, make a detailed understanding of laser-cluster processes desirable.

Much of the violent response of clusters to intense laser fields is related to the creation of a transient nanoplasma. A temporary resonant collective mode results strongly enhanced absorption, as has been demonstrated in simulations [11] as well as in experiments through increased yields of high-z ions [12], electrons [13,14] and x rays [15] for optimal pulse conditions. When present, plasmon-enhanced coupling is more effective than higher order nonlinear absorption effects [16]. The energy capture results from resonant driving of quasifree electrons, either inherent to the system or created through inner ionization, over a transiently critical ionic charge density $\rho_{\mathrm{crit}} = 3m_e\epsilon_0\omega_{\mathrm{las}}^2/e$. Because of strong field amplification at resonance also the asymmetry of the electron emission is increased, as has been observed on large ($N \sim 10^5$) noble-gas clusters [13]. The enhanced asymmetry was traced back to the polarization field at the cluster surface, which supports emission and most additional acceleration of electrons along the laser polarization.

In this contribution we investigate the electron emission from medium-sized *metal* clusters and find three key results: First, the experiments reveal an enhanced asymmetry of the electron emission at resonance. Although asymmetric electron emission has also been observed in previous experiments on large noble-gas cluster, we find that the mechanisms are fundamentally different in the size regime investigated here. Second, the asymmetry is electron energy dependent. The alignment along the laser polarization axis is maximal for the highest electron energies. Third, our analysis of the simulations reveals a so-far unresolved acceleration process described in the following: Upon laser excitation highly excited bound electrons with deflections significantly larger than the cluster radius are produced. They can be dynamically accelerated by the plasmon-enhanced polarization field during a final passage through the cluster. Therefore the parameter $s = \mathbf{v}_e \cdot \mathbf{p}$ has to fulfill certain conditions, where $\mathbf{v}_e$ is the velocity of the accelerated electron and $\mathbf{p}$ is the polarization created by the plasmon. Electrons can experience continuous energy gain for three plasmon half-cycles for $s < 0$ during their approach to the cluster, $s > 0$ for the transit through, and $s < 0$ for the escape from the cluster. This resulting cascadelike acceleration leads to substantial redistribution of collectively absorbed energy to single emitted electrons (multiplasmon deexcitation). As only certain trajectories meet these conditions for high gain, energetic electrons are ejected from the cluster in a subcycle burst.

The experiments are performed on neutral gas-phase silver clusters in the diameter range of $d = 3.4 \pm 0.8$ nm (500–2000 atoms), produced with a magnetron sputtering gas aggregation source. A beam of noninteracting clusters is delivered from the double differentially pumped molecular beam apparatus and irradiated with pairs of 100 fs laser pulses ($\lambda = 800$ nm, 2.5 mJ each, adjustable delay Δt) in a pump-probe type setup. The laser intensity is controlled by a movable $f/33$ focusing lens. Further details of the cluster generation and the laser system are described elsewhere [17]. Electron spectra are recorded by field-free time-of-flight measurements using a MCP detector and a GHz multiscaler card. The experimental time resolution allows discrimination of high-energy photons over electrons up to ~100 keV. To investigate the angular asymmetry, spectra have been measured with laser polarizations parallel ($E_{||}$) and perpendicular ($E_{\perp}$) with respect to the electron drift tube; cf. Fig. 1(a).

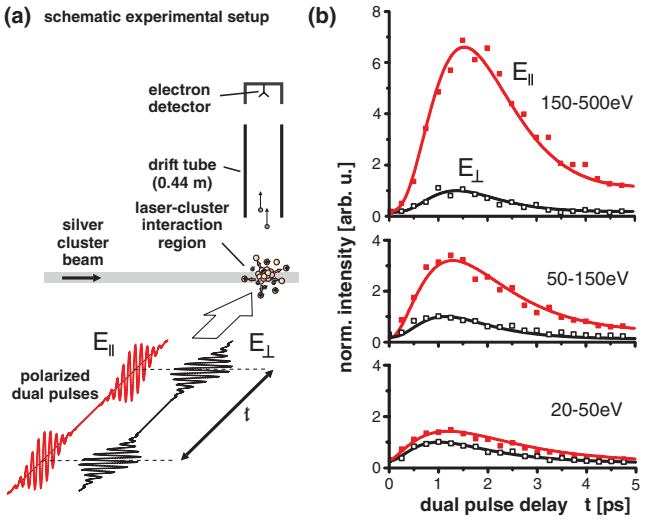

FIG. 1 (color). Photoelectron spectra from Ag_N upon excitation with dual 100 fs laser pulses at 8×10^{13} W/cm^2 for parallel ($E_{||}$) and perpendicular ($E_\perp$) laser polarization, see (a). The integrated signals for three electron energy intervals (as indicated) and normalized to the maximum obtained for $E_\perp$ (b).

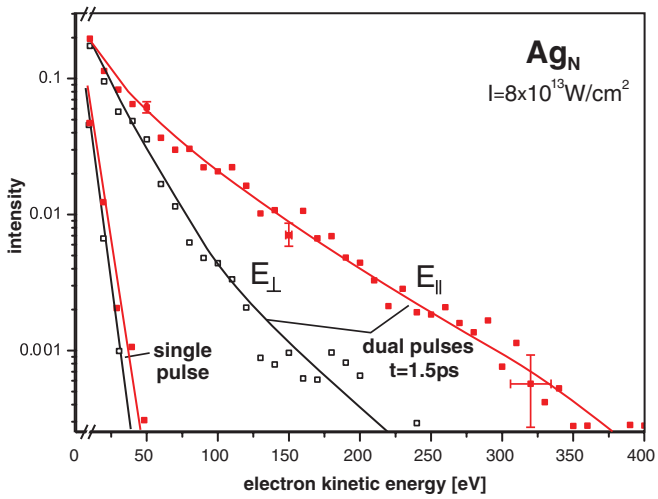

FIG. 2 (color). Angular-resolved photoelectron spectra for single vs resonant dual-pulse excitation. In the dual-pulse case significantly higher energies and a nonisotropic distribution are observed. The emission in favor of $E_{||}$ (closed symbols) is increasing with energy.

Irrespective of the direction of the emission the integrated electron intensities, shown for three selected energy intervals in Fig. 1(b), are maximal around delays $\Delta t \simeq 1.5$ ps. This optimal delay characterizes the necessary cluster expansion to reach critical density for resonant absorption. The strong delay dependence of angular integrated electron yields has already been observed in our previous measurements [14]. In the present results the electron emission exhibits a pronounced nonisotropic nature; see Fig. 1(b). Moreover, the angular asymmetry strongly depends on the electron energy. At the optimum delay the intensity ratio resulting from $E_{||}$ vs $E_\perp$ increases from 1.5 for the low-energy window to 6.5 for the high-energy window, reflecting enhanced directional preference of energetic electrons along the laser polarization axis. The shift of the peaks to longer delays with increasing electron energy can reasonably be explained by the size distribution in the cluster beam [18]. Further insight into the role of the resonance enhancement is gained from the fully resolved photoelectron energy spectra; see Fig. 2. Dual pulses with the optimal separation induce substantially higher electron yields as well as an order of magnitude increase in the electron energies over the single-pulse results. A maximum kinetic energy of 350 eV is observed for $E_{||}$ excitation. In addition, the distinct gap between the dual-pulse spectra for $E_{||}$ and $E_\perp$ beyond 50 eV indicates substantial increase of the alignment to the laser polarization with energy. Similar trends are observed for a wide intensity range (3×10^{13}–3×10^{14} W/cm^2). The increase in directional asymmetry at higher electron energies is produced by dynamic polarization field-assisted acceleration at resonance, as shown below via simulations. In contrast, nonresonant or single-pulse excitation results in lower electron energies and little angular preference.

We investigate the electron emission numerically by simulating the microscopic interaction process on the basis of a semiclassical kinetic approach. Sodium clusters serve as model systems, as corresponding calculations on silver with sufficient resolution are beyond the capability of present computers. Starting from the Thomas-Fermi ground state, valence electrons are propagated according to the Vlasov-Uehling-Uhlenbeck scheme by use of the test-particle method [19] incorporating mean-field effects (Coulomb interaction, exchange and correlation effects in local-density approximation) and binary electron-electron collisions (screened electron potential, cross sections from partial wave analysis, energy blocking) [20,21]. As we consider a highly nonlinear process with thermal excitations well beyond the spacing of energy levels the semiclassical approximation is justified. The electron dynamics is coupled to atomic ions via pseudopotentials. We consider icosahedral clusters Na_{147} irradiated by pairs of linearly polarized laser pulses ($\tau = 25$ fs, $\lambda = 800$ nm, $I = 8 \times 10^{12}$ W/cm^2). The reduced laser intensity is chosen because only one active electron per atom is treated explicitly. Nevertheless, the basic features and dynamical details of the laser-cluster interaction are recovered, as we show below.

Excitations with a single pulse only (a), with dual pulses having the optimal delay for resonant excitation (b), and a longer nonresonant pulse separation (c) lead to distinct features in the photoemission profiles; see Fig. 3. Note, in the simulation the optimal delay is shorter than in the experiments by a factor of about 4, as less relative expansion is required and the nuclei have smaller inertia. For resonant dual-pulse excitation (b) a strongly increased electron yield and significantly higher kinetic energies are found, in qualitative agreement with the measurements; cf. Fig. 2. The simulations predict maximal asymmetry of

the angular distribution for the resonant case, similar to the trends reported for lower intensity [22], and enhanced alignment of energetic electrons along the laser polarization axis. The maximum electron energy increases from 12 to roughly 47 eV: This value is 100 times larger than the ponderomotive energy. The enhancement degrades for optical delays that deviate substantially from the optimal value, see the spectrum obtained far off resonance as exemplarily shown in Fig. 3(c).

As the experimental trends are qualitatively reproduced we now focus on details of the electron dynamics at resonance from the simulation shown in Fig. 3(b). During the impact of the second pulse the energy absorption is governed by resonant plasmon excitation, i.e., collective driving of electrons orbiting inside the cluster. At the turning points of each plasmon cycle a portion of previously cluster-confined electrons is pulled beyond the cluster surface and experiences acceleration through the polarization repulsion. This repulsion corresponds to the polarization pressure reported for noble-gas clusters [13]. In our scenario we find that directly ejected electrons are unlikely to overcome the space-charge barrier, as the laser field partially counteracts the energy gain from polarization forces (electrons are emitted at most unfavorable phase). Therefore the direct mechanism mainly produces highly excited but still bound states.

It turns out that rescattering of highly excited states on the cluster potential is crucial for the asymmetric emission and the production of energetic electrons at resonance. A trajectory analysis reveals the following: Highly excited electrons can experience significant energy gain from the evolving resonance-enhanced polarization field during a final transit through the cluster. Therefore the projection of the electron velocity $\mathbf{v}_e$ on the plasmon induced polarization $\mathbf{p}$ has to meet certain conditions, which can be expressed by the projection parameter $s = \mathbf{v}_e \cdot \mathbf{p}$. For $s < 0$ during the approach to, as well as the escape from, the cluster, and $s > 0$ during the transit of the rescattered electron through the cluster, we find three steps of energy gain. Each on a time scale of half a plasmon cycle, as schematically depicted in Fig. 4(b) (from left to right). Continuous energy capture requires a flipping of the polarization, as the orientation of the polarization field is reversed in the cluster. In the optimal case electrons enter and exit the cluster near zero plasmon excursion. According to these constraints energetic electrons are only ejected in narrow time windows. This is clearly reflected in the camlike bursts within the time and energy resolved spectra for laser-aligned emission; see Fig. 4(a). Direct emission [broad low-energy contribution in Fig. 4(a)] also contrib-

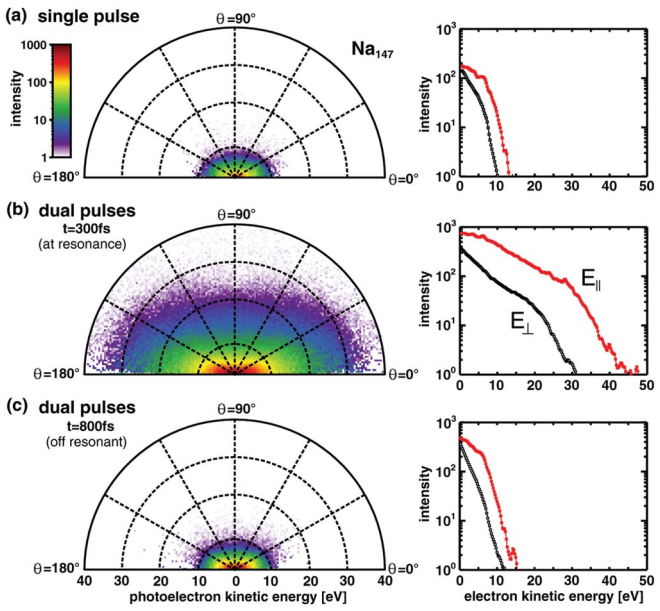

FIG. 3 (color). Calculated angular-resolved photoelectron spectra of Na_{147} for single-pulse (a) and dual-pulse laser excitations at optimal (b) and a longer nonresonant delay (c). In the polar spectra (left column) the emission angle θ is given with respect to the laser polarization axis. Cuts through the contours for $E_{\parallel}$ and $E_{\perp}$ (right column) represent simulated photoelectron spectra in accordance with the experimental setup.

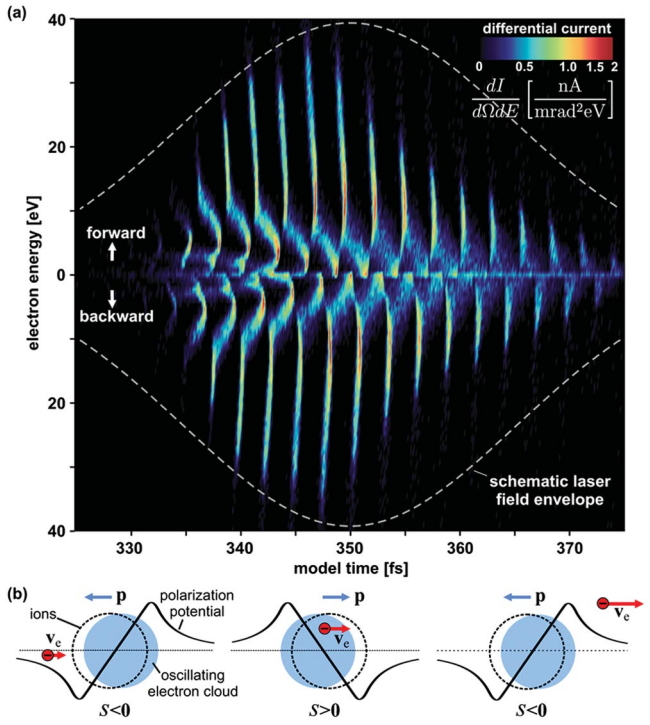

FIG. 4 (color). (a) Laser-aligned electron emission from Na_{147} during the second pulse extracted from the simulation in Fig. 3(b). The differential current corresponds to an average over a cone ($\Omega = 0.2\pi$). The emission time was measured at $r = 10$ nm (actual cluster radius $\simeq 2$ nm). Forward and backward emission is shifted by half a laser period. The data represent a statistical average. (b) Schematics of SPARC: At resonance the dynamical flipping of the polarization potential allows for efficient cascadelike acceleration of highly excited electrons upon their transit through the cluster (from left to right). For optimal acceleration the projection parameter $s = \mathbf{v}_e \cdot \mathbf{p}$ (see text) has to change sign as indicated in the three steps.

utes to the spectra but degrades quickly due to the increase of the cluster charge. More than half of the emission probability shown in Fig. 4(a) is concentrated in the sharp cam structure. It should be noted that the resulting subcycle bursts of energetic electrons can be resolved only in the vicinity of the clusters as dispersion leads to rapid spatial broadening.

The identified dynamical acceleration scheme, which we call surface-plasmon-assisted rescattering in clusters (SPARC), leads to efficient energy transfer from the plasmon into the electron emission. It can be interpreted as multiplasmon deexcitation rather than as a damping mechanism, as energy is redistributed into selected single particle channels. Electrons that are accelerated by the SPARC process can overcome the space-charge barrier even for high cluster ionization. Since the laser oriented momentum component of rescattered electron is increased preferentially, the resulting emission exhibits an enhanced asymmetry. As optimal acceleration is clearly associated to high polarization fields, the mechanism is mostly effective at resonance. For the Na_{147} simulation we find a peak field strength at the cluster center of 35 GeV/m, a factor of 5 larger than the laser field.

In conclusion, we have measured the angular and energy resolved photoemission from silver clusters, finding enhanced laser-aligned emission of energetic electrons at resonance. Simulations on Na_{147} as model system yield the same trends. They reveal the significance of SPARC for the production of energetic electrons. This polarization field-assisted acceleration requires a full passage of excited electrons through the cluster. Although our study is focused on medium-sized clusters, we suspect the SPARC mechanism is also important for slightly larger systems if the mean-free path of highly excited electrons is comparable to the cluster size. The selectivity of the SPARC mechanism to a particular class of trajectories results in the emission of subcycle bursts of energetic electrons. Future experiments with phase-locked few-cycle pulses (tuned to the resonance of the cluster) would be promising to resolve the rescattering mechanism and may open the possibility to generate trains of directed and energetic electrons already at moderate intensities. Such miniaturized electron sources would be interesting for nanoscience and femtochemistry, e.g., to probe structural features or dynamical processes of nanoparticles (being close to or attached to the cluster) with extremely high temporal resolution.

The authors gratefully acknowledge financial support by the Deutsche Forschungsgemeinschaft within the Sonderforschungsbereich No. 652. Computing time was provided by the High Performance Computing Center for North Germany (HLRN). We thank J. Köhn and S. Göde for assistance. One of the authors (T. F.) gratefully acknowledges enlightening discussions with T. Brabec.

*Electronic address: thomas.fennel@uni-rostock.de
Present address: Department of Physics, University of Ottawa, 150 Louis Pasteur, K1N 6N5 Ottawa, Canada.

[1] U. Saalmann, Ch. Siedschlag, and J. M. Rost, J. Phys. B **39**, R39 (2006).
[2] T. Ditmire, R. A. Smith, J. W. G. Tisch, and M. H. R. Hutchinson, Phys. Rev. Lett. **78**, 3121 (1997).
[3] E. Springate, S. A. Aseyev, S. Zamith, and M. J. J. Vrakking, Phys. Rev. A **68**, 053201 (2003).
[4] V. Kumarappan, M. Krishnamurthy, and D. Mathur, Phys. Rev. A **66**, 033203 (2002).
[5] A. McPherson, B. Thompson, A. Borisov, K. Boyer, and C. Rhodes, Nature (London) **370**, 631 (1994).
[6] E. M. Snyder, S. A. Buzza, and A. W. Castleman, Jr., Phys. Rev. Lett. **77**, 3347 (1996).
[7] T. Ditmire *et al.*, Nature (London) **386**, 54 (1997).
[8] Y. Fukuda *et al.*, Phys. Rev. A **67**, 061201(R) (2003).
[9] C. Jungreuthmayer, M. Geissler, J. Zanghellini, and T. Brabec, Phys. Rev. Lett. **92**, 133401 (2004).
[10] T. Ditmire *et al.*, Nature (London) **398**, 489 (1999).
[11] E. Suraud and P. G. Reinhard, Phys. Rev. Lett. **85**, 2296 (2000); U. Saalmann and J.-M. Rost, Phys. Rev. Lett. **91**, 223401 (2003); Ch. Siedschlag and J.-M. Rost, Phys. Rev. A **71**, 031401(R) (2005); T. Martchenko, Ch. Siedschlag, S. Zamith, H. G. Muller, and M. J. J. Vrakking, Phys. Rev. A **72**, 053202 (2005); I. Last and J. Jortner Phys. Rev. A **60**, 2215 (1999).
[12] E. Springate, N. Hay, J. W. G. Tisch, M. B. Mason, T. Ditmire, J. P. Marangos, and M. H. R. Hutchinson, Phys. Rev. A **61**, 044101 (2000); M. A. Lebeault, J. Viallon, J. Chevaleyre, C. Ellert, D. Normand, M. Schmidt, O. Sublemontier, C. Guet, and B. Huber, Eur. Phys. J. D **20**, 233 (2002); T. Döppner, Th. Fennel, T. Diederich, J. Tiggesbäumker, and K. H. Meiwes-Broer, Phys. Rev. Lett. **94**, 013401 (2005).
[13] V. Kumarappan, M. Krishnamurthy, and D. Mathur, Phys. Rev. A **67**, 043204 (2003).
[14] T. Döppner, Th. Fennel, P. Radcliffe, J. Tiggesbäumker, and K. H. Meiwes-Broer, Phys. Rev. A **73**, 031202(R) (2006).
[15] E. Lamour, C. Prigent, J. P. Rozet, and D. Vernhet, Nucl. Instrum. Methods Phys. Res., Sect. B **235**, 408 (2005).
[16] T. Taguchi, Th. M. Antonsen, Jr., and H. M. Milchberg, Phys. Rev. Lett. **92**, 205003 (2004); P. Mulser, M. Kanapathipillai, and D. H. H. Hoffmann, Phys. Rev. Lett. **95**, 103401 (2005); M. Kundu and D. Bauer, Phys. Rev. Lett. **96**, 123401 (2006).
[17] T. Döppner, Th. Fennel, P. Radcliffe, J. Tiggesbäumker, and K.-H. Meiwes-Broer, Eur. Phys. J. D **36**, 165 (2005).
[18] Larger clusters yielding the fastest electrons need slightly more time to expand to their critical radius.
[19] 10^4 samples per el., 257^3 grid points, 1 Å mesh spacing.
[20] Th. Fennel, G. F. Bertsch, and K. H. Meiwes-Broer, Eur. Phys. J. D **29**, 367 (2004).
[21] E. Giglio, P. G. Reinhard, and E. Suraud, J. Phys. B **33**, L333 (2000).
[22] E. Giglio, P. G. Reinhard, and E. Suraud, Phys. Rev. A **67**, 043202 (2003).